Liquid−Solid Phase Equilibria and Thermodynamic Modeling for Binary Organic Carbonates

Michael S. Ding*

Army Research Laboratory, 2800 Powder Mill Road, Adelphi, Maryland 20783

Temperature−composition values of liquid−solid equilibrium were measured calorimetrically and tabulated for 10 binary solutions of these 5 organic carbonates: ethylene carbonate, propylene carbonate, dimethyl carbonate, ethyl methyl carbonate, and diethyl carbonate. Further, heat capacity (C_p) and temperature (T_m) and enthalpy ($\Delta_{fus}H$) of fusion were measured for the five carbonates, with the C_p values fitted with polynomial functions. Based on these T_m and $\Delta_{fus}H$ values and polynomial functions of C_p, the binary phase diagrams were fitted with thermodynamic nonideal solution models for an evaluation of the model parameters. The results of the evaluation were tabulated and discussed as an indication of the nature and strength of the molecular interactions between different carbonates. These interactions were shown to determine many of the important features of the binary phase diagrams.

Introduction

Organic carbonates have long been considered as the most suitable solvents for electrolytes of lithium-ion batteries due to their exceptional chemical stability and other favorable physicochemical properties.[1,2] Of critical importance among the latter is the lower-temperature boundary of the liquid range of a carbonate, which places a limit on the low-temperature operation of the battery in which it serves as the electrolyte solvent. This boundary is the melting point for a pure carbonate and the liquidus temperature for a carbonate mixture. Owing to the significant lowering of the melting point of a carbonate when mixed with a second one, in addition to other favorable changes in properties, liquid−solid phase diagrams have been experimentally mapped and published in graphical form for all the binary combinations of these five common carbonates: ethylene carbonate (EC), propylene carbonate (PC), dimethyl carbonate (DMC), ethyl methyl carbonate (EMC), and diethyl carbonate (DEC), of which EC and PC are cyclic in molecular structure and DMC, EMC, and DEC are linear.[3−5] Subsequently, these measured phase diagrams have been thermodynamically modeled, first qualitatively with a regular solution model for the purpose of understanding the underlying molecular mechanisms,[6] and then quantitatively with a nonregular solution model for the purpose of predicting a ternary phase diagram of EC + PC + DMC.[7]

The aim of this work is first to tabulate the numerical values of temperature−composition for the phase diagrams of the 10 binary carbonates that have only been published graphically. These values comprise those measured anew and those measured in the previous studies.[3,4] It is second to list the temperature and enthalpy of fusion and the heat capacity in functional form for the five carbonate components. It is third to describe thermodynamic modeling of the binary phase diagrams in which parametrized nonideal solution models were optimized against the measured temperature−composition values, to tabulate the resulting parameter values, and to briefly discuss the molecular mechanisms for some observed trends in the phase diagrams in terms of the evaluated model parameters.

* E-mail: mding@arl.army.mil.

Experimental Section

Experimental Determination of Phase Diagrams. The 10 binary phase diagrams of the 5 carbonates EC, PC, DMC, EMC, and DEC have previously been determined using a differential scanning calorimeter (DSC 7 by Perkin-Elmer).[3,4] However, in light of a successful determination in a more recent work of the eutectic temperatures of PC + EC and PC + DEC binaries with very PC-rich samples,[8,9] the eutectic temperatures of PC + DMC and PC + EMC binaries and the solubility curves of EC, EMC, and DEC in PC were similarly determined in this work. These extended solubility curves, in combination with the accurately determined eutectic points, allow the eutectic compositions to be accurately determined. The addition of these solubility curves and eutectic points to the experimental data set for the thermodynamic fitting greatly improved the quality of the model parameters thus evaluated in this study.

The additional determinations were carried out on samples of carbonates the source and the preparation of which were the same as in a previous work.[8] Measurement of liquidus and eutectic temperatures was carried out using a modulated differential scanning calorimeter (MDSC 2920 by TA Instruments). Liquid nitrogen was used for cooling the sample stage, and the sample was sealed in a pair of aluminum pan and lid (0219-0062 by Perkin-Elmer). For the actual determination of the characteristic temperatures, a sample was first made to crystallize by cooling it to a temperature well below its eutectic point and then heated at a rate of 2 K min^{-1} without modulation through its eutectic and liquidus temperatures. For the pure solvents, the melting point was determined as the onset of the heat absorption due to the melting, and the enthalpy of fusion by integrating the absorption peak against baseline. For the solvent mixtures, the eutectic point was determined as the onset of the heat absorption at the solidus transition and the liquidus temperature at the peak point at the liquidus transition. The uncertainty was

10.1021/je034134e CCC: $27.50
Published on Web 12/02/2003

Table 1. Experimental Values for the Temperature, *T*, of Liquidus, Solidus, and Solid−Solid Phase Transitions at Different Values of Mole Fraction, *x*, for the Binary Organic Carbonates Containing Dimethyl Carbonate as the Common Component

x_1	*T*/K (liquidus)	*T*/K (solidus)	*T*/K (solid−solid)	x_1	*T*/K (liquidus)	*T*/K (solidus)	*T*/K (solid−solid)	x_1	*T*/K (liquidus)	*T*/K (solidus)	*T*/K (solid−solid)
Ethylene Carbonate (1) + Dimethyl Carbonate (2)											
0.0000	278.2		218.4	0.2489	266.4	264.2	218.1	0.6513	289.4	264.1	217.8
0.0501	274.8	264.2	218.3	0.2768	265.3	264.2	217.9	0.7009	291.6	264.2	217.9
0.0770	273.6	264.2	218.3	0.2995		264.2	217.9	0.7505	295.1	264.4	218.0
0.1011	272.7	264.2	218.3	0.3478	268.4	264.2	217.5	0.7988	297.5	264.2	218.0
0.1258	271.6	264.2	218.3	0.4016	271.7	264.2	217.6	0.8467	299.8	264.1	217.9
0.1515	270.7	264.3	218.1	0.4505	276.0	264.2	217.7	0.8898	303.3	263.8	218.0
0.1761	269.4	264.2	218.2	0.4987	279.4	264.2	217.8	0.9499	307.3	263.9	
0.2013	268.8	264.4	218.4	0.5505	283.8	264.3	218.0	1.0000	311.2		
0.2246	267.3	264.2	218.1	0.6006	286.5	264.4	217.9				
Dimethyl Carbonate (1) + Diethyl Carbonate (2)											
0.0000	198.2			0.2486	214.0	193.4		0.7012	258.3	193.2	218.4
0.0249	198.2	193.1		0.3002	221.7	193.2	218.3	0.7511	261.9	193.1	218.4
0.0506	197.1	193.2		0.3484	227.7	193.2	218.7	0.7998	265.5	193.3	218.5
0.0737		193.3		0.3996	232.2	193.1	218.3	0.8489	268.9	193.2	218.5
0.0995		193.2		0.4523	238.4	193.2	218.4	0.8986	271.4	193.1	218.4
0.1260		193.3		0.5000	242.4	193.1	218.4	0.9510	275.0	192.9	218.4
0.1500		193.3		0.5496	247.5	193.3	218.4	1.0000	278.2		218.3
0.1769		193.1		0.6008	251.0	193.2	218.4				
0.2024	206.9	193.2		0.6495	254.9	193.1	218.5				
Dimethyl Carbonate (1) + Propylene Carbonate (2)											
0.0000	220.3			0.2499	225.4		218.8	0.6621	261.2		218.7
0.0076		210.0		0.3003	232.2		218.8	0.6996	263.2		218.8
0.0189		210.3		0.3496	237.7		218.7	0.7501	265.9		218.7
0.0311		210.2		0.4027	243.0		218.7	0.7993	268.2		218.8
0.1118	201.4			0.4498	246.9		218.7	0.8501	270.6		218.7
0.1385	206.6			0.5011	250.5		218.7	0.8998	272.7		218.7
0.1678	211.6			0.5521	254.6		218.8	0.9491	274.9		218.7
0.1998	217.2			0.6071	257.5		218.7	1.0000	277.2		218.7

estimated to be 0.5 K in the measurement of eutectic (or solidus) and melting temperatures and 1 K in the measurement of liquidus temperature.

Experimental Determination of Heat Capacities. Heat capacities, C_p, of the carbonates were determined on the MDSC with samples crimp-sealed in a pair of aluminum pan and lid.[8] For a measurement, a sample was first equilibrated at 173 K and then heated at 1 K min^{-1} to 323 K with a modulation of 0.5 K amplitude and 60 s period. The temperature range was such that the lower limit was below the lowest eutectic temperature of the binary phase diagrams and the upper limit was above the highest melting point of the carbonate components. For calibration, a piece of Al_2O_3 crystal disk of 21.8 mg was measured in the same temperature range under the same conditions. This C_p curve, together with the standard values published,[10] was used to correct the C_p values of the carbonate samples at different temperatures. These corrected values were further fitted with polynomial functions for use in the thermodynamic fitting of binary phase diagrams.

Computational Optimization of Thermodynamic Models. Programs for fitting the measured phase diagrams with thermodynamic nonideal solution models were written in Mathematica 4 (Wolfram Research) and run on a Pentium 4 personal computer. The models contained up to three fitting parameters in the expression for the excess Gibbs energy of mixing. The target function to be minimized was the sum of the squared differences between the measured solvent compositions and the modeled ones for different temperatures. Equal weight was given to each measured point except those lying on the solidus line for the PC-containing binaries, to which more weight was given due to the high consistency in the measurement of these points and to the difficulty of obtaining more points at less PC-rich compositions due to the strong resistance of PC to crystallization.[3]

Results and Discussion

Liquid−Solid Phase Equilibria for Binary Carbonates. Temperature−composition values measured at liquid−solid equilibrium for the 10 binary carbonates are listed in Table 1 for those binaries with DMC as a component that exhibited a measurable solid−solid phase transition and in Table 2 for the rest of the binaries. They are also graphically plotted in Figure 1 together with the associated phase lines resulting from the thermodynamic modeling to show the general features of the phase diagrams and the closeness of the fit. It can be seen that although vastly different in detail, the phase diagrams of all the carbonates are of the simple eutectic type, showing them to be completely soluble in one another in the liquid state but insoluble in the solid state. It can also be seen, in a comparison of the phase diagrams containing EC as the common component as plotted in Figure 2a, that the lower-temperature liquid boundary shifts upward in the order of DMC, EMC, and DEC, contrary to the trend in the melting points of these linear carbonates. This observation was quite counterintuitive and thus significant in pointing out the right direction to the formulation of carbonate mixtures for low-temperature application.[4] It can also be observed, as exemplified by the phase diagrams of those binaries having DMC as the common component as plotted in Figure 2b, that a cyclic carbonate dissolves another cyclic more readily than another linear, and vice versa. These observations are manifestations of a higher degree of molecular compatibility between carbonates of the same cyclicity than of the opposite and, in the case of EC with the linear carbonates, of this molecular compatibility diminishing from DMC to EMC to DEC.[6]

Heat Capacity and Temperature and Enthalpy of Fusion of Carbonates. Heat capacities of the carbonates were measured mainly for use in the thermodynamic

Table 2. Experimental Values for the Temperature, *T*, of Liquidus and Solidus Phase Transitions at Different Values of Mole Fraction, *x*, for the Binary Organic Carbonates without a Measurable Solid−Solid Phase Transition

x_1	*T*/K (liquidus)	*T*/K (solidus)	x_1	*T*/K (liquidus)	*T*/K (solidus)	x_1	*T*/K (liquidus)	*T*/K (solidus)
Ethylene Carbonate (1) + Ethyl Methyl Carbonate (2)								
0.0000	219.4		0.3909	280.8	218.1	0.7334	294.8	218.1
0.0586		218.1	0.4408	281.2	218.2	0.7792	296.0	218.2
0.1144	256.4	218.2	0.4924	283.4	218.3	0.8265	299.0	218.2
0.1734	266.5	218.3	0.5410	285.5	218.3	0.8695	301.5	218.1
0.2296	266.1	218.2	0.5907	287.1	218.3	0.9128	304.3	217.8
0.2820	273.7	218.1	0.6409	290.1	218.2	0.9579	307.6	217.9
0.3393	277.8	218.5	0.688	292.2	218.2	1.0000	311.2	
Ethylene Carbonate (1) + Diethyl Carbonate (2)								
0.0000	198.2		0.3507	284.4	196.4	0.7012	296.6	196.5
0.0491		196.7	0.3988	285.0	196.6	0.7506	298.4	196.5
0.101	268.8	196.7	0.4503	287.5	196.5	0.7995	300.4	196.4
0.149	275.3	196.3	0.5017	290.3	196.5	0.8505	302.8	196.4
0.2015	278.8	196.5	0.5499	291.1	196.5	0.893	305.0	196.3
0.2479	280.4	196.6	0.602	292.8	196.5	0.9506	308.3	196.4
0.299	282.3	196.5	0.6498	294.9	196.5	1.0000	311.2	
Ethylene Carbonate (1) + Propylene Carbonate (2)								
0.0000	220.3		0.4504	265.6		0.7991	294.0	
0.0061		208.0	0.5005	270.6		0.8492	297.8	
0.0122		207.9	0.5506	273.9		0.8995	301.8	
0.0295		207.8	0.5965	279.8		0.9354	304.6	
0.3001	253.6		0.6499	284.0		1.0000	311.2	
0.3498	255.1		0.6999	288.2				
0.4003	257.1		0.7492	290.8				
Ethyl Methyl Carbonate (1) + Propylene Carbonate (2)								
0.0000	220.3		0.3497	198.5		0.7017	212.8	
0.0067		199.8	0.4008	201.4		0.7517	214.1	
0.0197		199.9	0.4504	204.0		0.7995	215.4	
0.0334		199.8	0.4993	206.0		0.8546	216.8	
0.1998	187.3		0.5511	207.9		0.8998	217.6	
0.2554	191.3		0.5996	209.7		0.9513	218.5	
0.3023	195.2		0.6485	211.9		1.0000	219.4	
Diethyl Carbonate (1) + Propylene Carbonate (2)								
0.0000	220.3		0.6005	189.4		0.8507	194.7	
0.0076		189.6	0.6499	190.8		0.8996	195.5	
0.0189		189.6	0.7024	191.9		0.9659	196.6	
0.0311		189.6	0.7503	192.9		1.0000	198.2	
0.5505	188.1		0.7984	194.1				
Dimethyl Carbonate (1) + Ethyl Methyl Carbonate (2)								
0.0000	219.4		0.3487	226.8	209.6	0.7506	262.0	209.0
0.0492	217.2	209.7	0.4014	233.9	209.6	0.7979	265.5	209.3
0.1022	215.0	209.6	0.4958	242.2	209.5	0.8484	268.4	209.1
0.1518	213.4	209.9	0.5507	247.0	209.4	0.9006	271.7	209.0
0.2004		209.1	0.5985	250.8	209.2	0.9399	273.7	208.6
0.2505	215.2	209.9	0.6478	254.6	208.8	1.0000	277.7	
0.2984	222.1	209.7	0.6978	258.7	208.6			
Ethyl Methyl Carbonate (1) + Diethyl Carbonate (2)								
0.0000	198.2		0.2262	190.0	184.4	0.6510	204.5	183.0
0.0247	197.3	183.4	0.2596	188.9	184.3	0.7001	206.7	182.9
0.0520	197.2	183.9	0.3000		184.5	0.7499	208.4	183.2
0.0723	196.1	184.2	0.3501		184.5	0.8000	210.5	183.1
0.1022	194.5	184.2	0.3991	191.4		0.8515	212.8	184.1
0.1251	194.3	184.5	0.4513	195.0	183.1	0.9001	215.1	184.0
0.1509	193.5	184.5	0.4990	197.1	183.1	0.9516	217.1	183.8
0.1751	192.2	184.5	0.5505	199.9	182.9	1.0000	219.4	
0.1994	191.1	184.7	0.5989	202.1	183.0			

modeling of the binary phase diagrams but not for providing accurate values for tabulation; the uncertainty in these measurements was estimated to be as high as 5% due to inherent limitations of the method and the procedures used. Therefore, the measured C_p values have not been tabulated here; instead, the constants in the polynomial functions that have been fitted to these measured values and used in the thermodynamic modeling are tabulated in Table 3 for an approximate representation of the heat capacities. In addition, the functions are plotted in Figure 3 to show the temperature dependence of and the relations among the heat capacities of the carbonates. For liquids below their melting points, the carbonates were supercooled as low as possible and measured for their C_p in subsequent heating, and heat capacities at lower temperatures where the supercooling could not be achieved without crystallization were linearly extrapolated from the measured values at higher temperatures. For solids in their superheated state above their melting points, the heat capacities were represented with linear functions with the same values as those of the corresponding solids at the melting points and with the same slopes as those of the corresponding liquids.[7,11] These extrapolations were necessitated by and used in the thermodynamic modeling and are not intended as estimates for the actual C_p values. The measured C_p values, despite their significant uncertainty, should have a high degree of internal consistency since they were all determined under the same conditions against the same

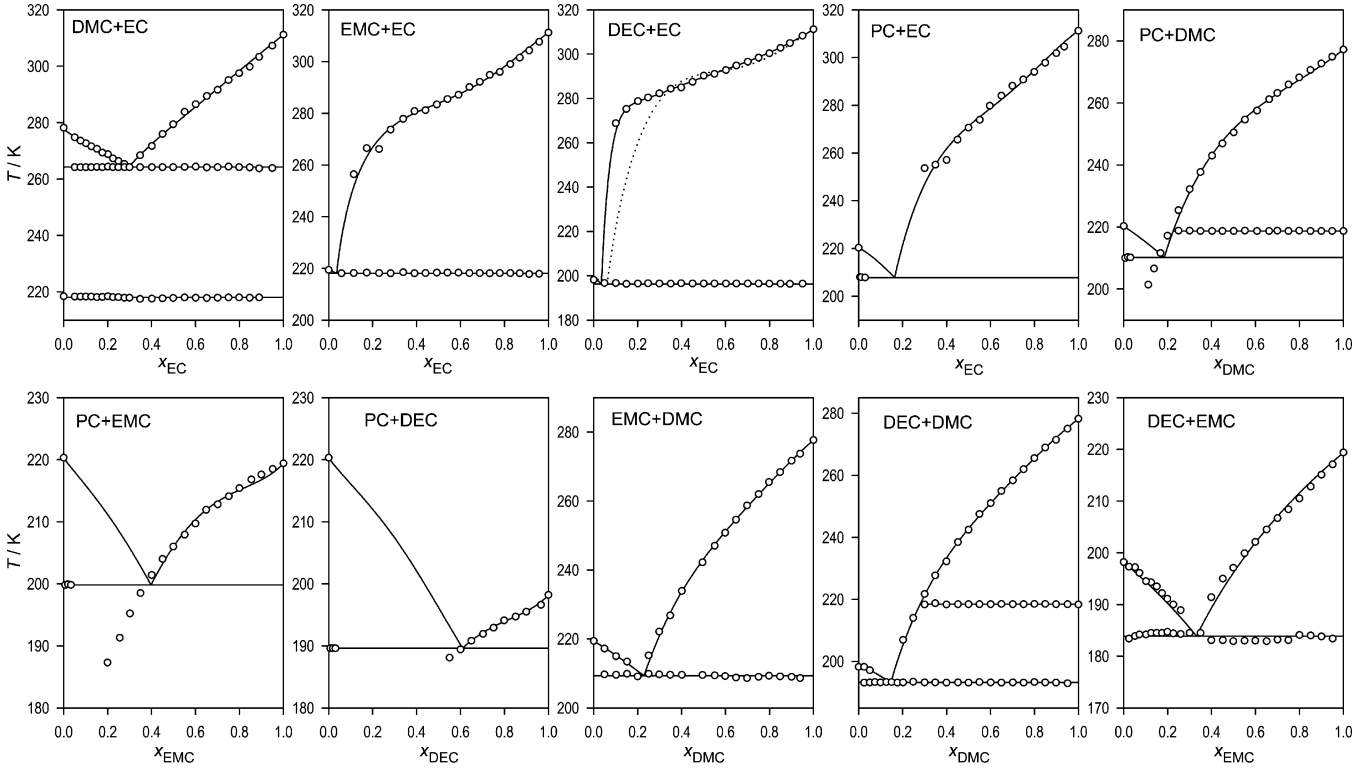

Figure 1. Experimentally determined phase diagrams (the open dots) for the 10 binary combinations of EC, PC, DMC, EMC, and DEC and their thermodynamic fit (the curves) with the nonideal solution models of eqs 1−5, with the parameter values listed in Table 4. The dotted curves in the DEC + EC phase diagram would result with a nonregular solution model (polynomial) instead of the nonideal solution model (exponential) actually used.

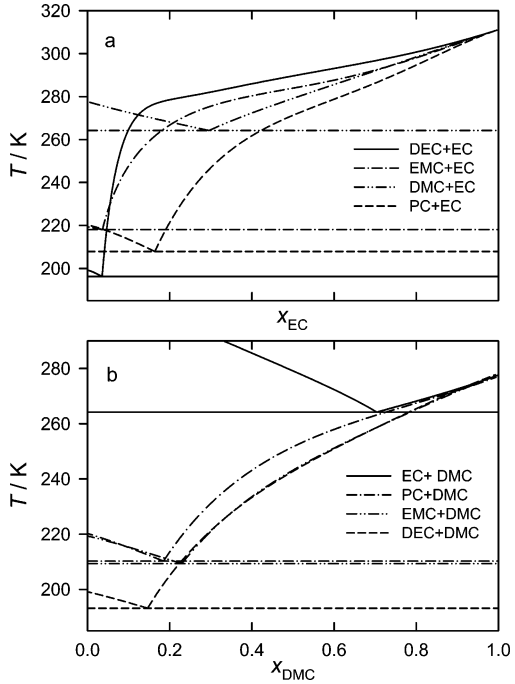

Figure 2. Comparison of phase diagrams for the binary carbonates containing as the common component EC (a) and DMC (b).

reference. These functions also yield reasonable values when compared to the published data;[12] for example, they give for liquid PC at 298.2 K a value of 153.6 J mol^{-1} K^{-1} against a published value of 167.6 J mol^{-1} K^{-1};[13] for liquid EC at 323.2 K, 136.2 J mol^{-1} K^{-1} against 133.9 J mol^{-1} K^{-1};[14] for solid EC at 298.2 K, 117.1 J mol^{-1} K^{-1} against 117.4 J mol^{-1} K^{-1};[13] and for liquid DEC at 294.2 K, 227.8 J mol^{-1} K^{-1} against 210.9 J mol^{-1} K^{-1}.[15]

Table 3. Heat Capacity C_p,[a] Melting Point T_m, and Enthalpy of Fusion $\Delta_{fus}H$ for the Common Organic Carbonates

	EC	PC	DMC[b]	EMC	DEC
formula	$C_3H_4O_3$	$C_4H_6O_3$	$C_3H_6O_3$	$C_4H_8O_3$	$C_5H_{10}O_3$
cyclicity	cyclic	cyclic	linear	linear	linear
T_m/K	311.2	220.3	278.2	219.4	198.2
$\Delta_{fus}H$/kJ mol^{-1}	13.02	8.960	11.58	11.24	9.24
C_p (liquid), a_0	1.0651	1.8634	1.2492	1.0943	1.0916
a_1	1.4882	−8.8749	1.9855	2.2044	2.845
a_2		41.062			
a_3		−51.439			
C_p (solid), a_0	−1.3355	−0.6951	2.8141	−0.6586	0.0051
a_1	24.09	13.142	−15.196	9.9732	6.5192
a_2	−94.804	−24.124	37.364		
a_3	147.55				
C_p (s.h. solid[c]), a_0	0.95561	0.59197	0.92673	1.0367	0.73366
a_1	1.4882	1.9789	1.9855	2.2044	2.845

[a] C_p/J mol^{-1} K^{-1} = $a_0 + a_1(T/10^3\ \text{K}) + a_2(T/10^3\ \text{K})^2 + a_3(T/10^3\ \text{K})^3$. [b] For C_p of DMC below its solid−solid phase transition at 220.1 K, the values for a_0, a_1, a_2, a_3, and a_4 are 271.76, −5638.2, 43952, −152041, and 197217, respectively. [c] s.h. solid stands for superheated solid, i.e., the solid phase of a carbonate above its melting point T_m.

As shown in Figure 3, the heat capacity of a carbonate in its solid state is always below that in its liquid state, as would normally be expected. However, an exception can be seen in DMC, which is the only one that displays two different phases in the solid state. As shown in the figure, the heat capacity is actually higher for the solid phase of lower temperature than of higher temperature and almost reaches the value of the liquid DMC at the solid−solid phase transition. Meanwhile, the enthalpy of the phase transition was quite low, which, in combination with the strong change in C_p, makes it reasonable to treat the transition as a second-order phase transition.

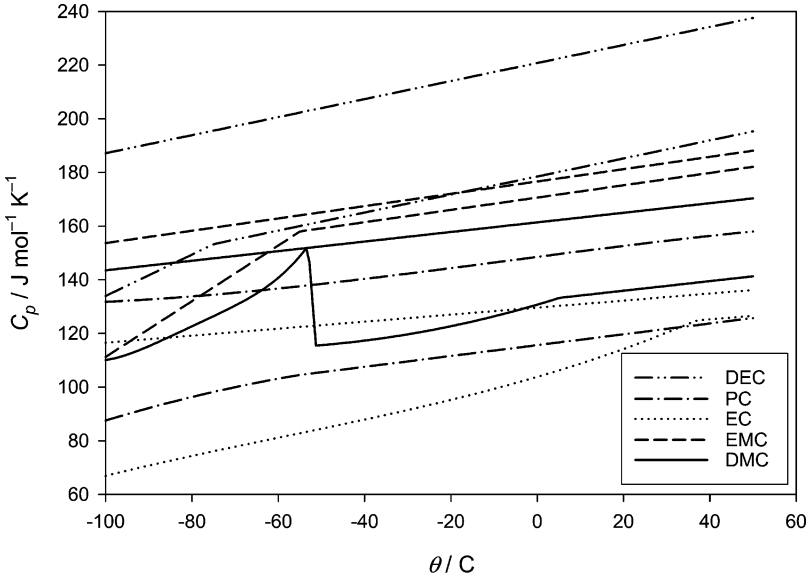

Figure 3. Heat capacity curves for the carbonates in liquid−solid pairs in the range of (−173 to 323) K, obtained by fitting polynomial functions to the measured C_p data where available, by linearly extrapolating the measured data to where data could not be measured, or, for solids in their superheated state, by linearly extending their C_p curves from their measured values at the melting points with the same slopes as those of their liquids. For each pair of curves, the upper one is for the liquid and the lower one for the solid.

Also listed in Table 3 are the measured values of temperature (T_m) and enthalpy ($\Delta_{fus}H$) of fusion that were used in the thermodynamic calculation. The T_m value agrees with the published ones within experimental error for EC[13,16] and DEC,[4] is about halfway in a 4 K span between the high and the low of the published values for PC,[16−18] and agrees closely with the generally accepted values for DMC and EMC.[4] The $\Delta_{fus}H$ value agrees well with the published ones for EC but is about 7% smaller than the published ones for PC.[13,16] The evaluation results for the model parameters in the thermodynamic fitting of a binary phase diagram were not very sensitive to the C_p, T_m, and $\Delta_{fus}H$ of the binary components but were affected strongly by the diagram pattern.

Thermodynamic Modeling. Thermodynamic nonideal solution models were fitted to the 10 measured binary phase diagrams for an evaluation of the model parameters[19] for a better understanding of the molecular mechanisms underlying the behavior of the carbonates in their liquid−solid phase equilibria[20] and for a greater ability to accurately predict ternary phase diagrams of carbonates.[7,19] The models assume a total absence of solubility of the carbonates in one another in their solid state, which, as evidenced by their measured phase diagrams shown in Figure 1,[3,4] should be a good approximation. They also assume that the part in Gibbs free energy of mixing in the liquid state due to change of entropy can be exclusively represented by the expression[19,20]

$$\Delta_{mix}G^{id} = RT(x_B \ln x_B + x_A \ln x_A) \quad (1)$$

where R is the gas constant, T is the temperature in Kelvin, and x_A and x_B are the mole fractions of the two components A and B. Thus, the Gibbs energy of mixing for a binary A + B in the liquid state can be written as

$$\Delta_{mix}G = \Delta_{mix}G^{id} + G^E + x_A\Delta_{fus}G_A + x_B\Delta_{fus}G_B \quad (2)$$

with the Gibbs energies of pure crystalline A and B as its reference. The Gibbs energy of fusion of A at temperature T is

$$\Delta_{fus}G_A = \Delta_{fus}H_A(1 - T/T_{m,A}) + \int_{T_{m,A}}^{T}(C_{p,A}^{l} - C_{p,A}^{s})\,dT - T\int_{T_{m,A}}^{T}(C_{p,A}^{l} - C_{p,A}^{s})\,d\ln T \quad (3)$$

where $\Delta_{fus}H$ is the enthalpy of fusion at the melting point T_m, and C_p^l and C_p^s are the heat capacities of A in its liquid and solid states at the temperature. The same equation serves to describe the Gibbs energy of fusion for B when all its A's are replaced by B's. The excess Gibbs free energy of mixing, G^E, renders the model of eq 2 nonideal and is expressed as[19]

$$G^E = x_Ax_B(a_0 + a_1x_B + a_2x_B^2) \quad (4)$$

for all but one of the binary carbonates. Not all the parameters a_0, a_1, and a_2 are always needed for eq 2 to produce a good fit to a measured phase diagram; therefore, according to whether one uses a zero, constant, linear, or quadratic term in eq 4, the resulting model is termed an ideal, regular, subregular, or nonregular solution model.[19,20] Despite its flexibility in fitting various phase diagrams,[19] the nonregular solution model was found inadequate in fitting a particular binary carbonate, EC + DEC, due to the unusual shape of the solubility curve of EC in DEC. Instead, the following expression was found to be far more suitable:

$$G^E = x_{DEC}x_{EC}[a_0 + a_1(1 - e^{a_2x_{EC}})] \quad (5)$$

As this nonpolynomial term makes unfit the use of *nonregular* solution for the description of the model utilizing the term, *nonideal* solution is used instead to cover all the thermodynamic models of this work.

For a simple eutectic binary A + B, eq 2 with a given set of numerical values for the parameters a_1, a_2, and a_3 of eq 4 or 5, together with the assumption of mutual insolubility in the solid state, uniquely determines a pair of composition values for the solubilities of A in B and of B in A at a certain temperature, that is,

$$x = f(T,a_0,a_1,a_2) \quad (6)$$

Table 4. Parameter Values[a] of a_1, a_2, and a_3 in the Nonideal Solution Models, Evaluated by Fitting the Models to the Measured Binary Phase Diagrams, and the Integral Gibbs Energy of Mixing, g,[b] for the Binary Organic Carbonates

	DEC + EC	EMC + EC	DMC + EC	PC + DEC	PC + EMC	PC + DMC	DEC + DMC	EMC + DMC	DEC + EMC	PC + EC
a_0	−3850.3	2595.6	2126.0	1449.5	938.83	−38.692	−269.38	−571.69	−223.51	−3099.6
a_1	6950.0	1053.7	−944.19	−1486.5	−852.03	2035.1	1194.7	1810.9	51.238	7974.8
a_2	−15.823	−2121.2	0	2626.4	2587	−407.60	−1216.4	−1461.8	0	−6825.8
g	492.4	414.4	275.7	249.0	214.8	142.8	−6.163	−17.46	−32.98	−193.3

[a] $G^E/\mathrm{J\ mol^{-1}} = (1-x)x[a_0 + a_1(1-\exp a_2 x)]$ for DEC + EC and $=(1-x)x(a_0 + a_1 x + a_2 x_2)$ for the rest, with x as the mole fraction of the second component as listed. [b] $g/(\mathrm{J\ mol^{-1}}) = \int_0^1 G^E\,dx$.

These two relations when plotted in the $x-T$ coordinates trace out the two solubility curves which meet at the eutectic point (x_e, T_e), in the process generating a complete solid−liquid phase diagram for the A + B binary.[6]

By reversing this process of building a phase diagram from a set of parameter values, a nonideal solution model can be optimized against a measured phase diagram for an evaluation of the parameters. This optimization has been achieved in this work by minimizing a target function consisting of sums of the squared differences between the measured values (T_i, x_i) and the model values [T_i, $f(T_i,a_0,a_1,a_2)$] and between the x-values of the two solubility curves at the measured eutectic point T_e:

$$S(a_0,a_1,a_2) = (\sum_i^{\mathrm{A}} + \sum_i^{\mathrm{B}})[f(T_i,a_0,a_1,a_2) - x_i]^2 + n(f^{\mathrm{A}} - f^{\mathrm{B}})^2(T_e,a_0,a_1,a_2) \quad (7)$$

where A and B denote the solubility curves of A in B and B in A, respectively, and n is the number of times by which the eutectic point has been measured at different compositions. Results of such optimization for the 10 measured phase diagrams of binary carbonates are plotted in Figure 1 against the measured phase points, the close fits of the models to the experimental data indicating a high degree of reliability in the model parameters thus evaluated. These parameter values are listed in Table 4 for a_1, a_2, and a_3, together with the values of integral excess Gibbs energy of mixing g obtained by integrating the Gibbs energy in the whole composition range using the corresponding parameter values. This integral property can be seen as an indication of the nature and the strength of the intermolecular forces between the two component molecules in the liquid state; a high positive value reflects a much weaker attraction between the two different molecules than the average attractive forces between the molecules of the same kind, and a high negative value, a much stronger attraction.[20] Thus, a comparison of the first three g-values in Table 4 with their corresponding phase diagrams in Figure 2a shows that the upward shift of the solubility curve of EC in the linear carbonates in the order of DMC, EMC, and DEC is a result of the increasingly weaker attraction between the molecules of EC and the linear carbonates. Clearly, it is the molecular compatibility between the two components that determines the solubility of one in the other, not their melting points.[6] For the same reason, the higher solubility of DMC in EMC and DEC than in EC and PC shown in Figure 2b is a result of the higher molecular compatibility between two linear carbonates than between a linear and a cyclic carbonate, the g-values being both negative for the former and positive for the latter as seen in Table 4.

Conclusions

Temperature−composition values of liquid−solid equilibrium were measured calorimetrically and tabulated for 10 binary solutions of these 5 organic carbonates: EC, PC, DMC, EMC, and DEC. Further, these binary phase diagrams were closely fitted with thermodynamic nonideal solution models, based on the measured values of heat capacity and temperature and enthalpy of fusion of the five carbonate components, for an evaluation of the model parameters. The evaluation results, combined with the phase diagrams, indicated that many of the important features of the phase diagrams are determined mainly by the molecular compatibility between the component carbonates. More specifically, a cyclic carbonate dissolved another cyclic more readily than another linear, and vice versa. Of particular interest and importance is the series of DMC, EMC, and DEC with EC, where these linear carbonates dissolved EC with increasing difficulty resulting in decreasing expansions of the liquid regions of the phase diagrams into low temperature, manifesting a diminishing molecular compatibility of EC with the linear carbonates from DMC to EMC to DEC.

Supporting Information Available:

Tables of experimental molar heat capacities of organic carbonates at different temperatures. This material is available free of charge via the Internet at http://pubs.acs.org.

Literature Cited

(1) Ehrlich, G. M. Lithium-ion batteries. In *Handbook of Batteries*, 3rd ed.; Linden, D., Reddy, T. B., Eds.; McGraw-Hill: New York, 2002.

(2) Ding, M. S. Electrolytic Conductivity and Glass Transition Temperature as Functions of Salt Content, Solvent Composition, or Temperature for $LiPF_6$ in Propylene Carbonate + Diethyl Carbonate. *J. Chem. Eng. Data* **2003**, *48*, 519−528.

(3) Ding, M. S.; Xu, K.; Jow, T. R. Liquid−Solid Phase Diagrams of Binary Carbonates for Lithium Batteries. *J. Electrochem. Soc.* **2000**, *147*, 1688−1694.

(4) Ding, M. S.; Xu, K.; Zhang, S.-S.; Jow, T. R. Liquid/Solid Phase Diagrams of Binary Carbonates for Lithium Batteries, Part II. *J. Electrochem. Soc.* **2001**, *148*, A299−A304.

(5) Ding, M. S.; Xu, K.; Jow, T. R. Phase Diagram of EC−DMC Binary System and Enthalpic Determination of Its Eutectic Composition. *J. Therm. Anal. Calorim.* **2000**, *62*, 177−186.

(6) Ding, M. S. Thermodynamic Analysis of Phase Diagrams of Binary Carbonates Based on a Regular Solution Model. *J. Electrochem. Soc.* **2002**, *149*, A1063−A1068.

(7) Liu, Z.-K. Thermodynamic Modeling of Organic Carbonates for Lithium Batteries. *J. Electrochem. Soc.* **2003**, *150*, A359−A365.

(8) Ding, M. S. Liquid Phase Boundaries, Dielectric Constant, and Viscosity of PC−DEC and PC−EC Binary Carbonates. *J. Electrochem. Soc.* **2003**, *150*, A455−A462.

(9) Angell, C. A.; Boethm, L.; Oguni, M.; Smith, D. L. Far IR Spectra and Heat Capacities for Propylene Carbonate and Propylene Glycol and the Connection to the Dielectric Response Function. *J. Mol. Liq.* **1993**, *56*, 275−286.

(10) Ditmars, D. A.; Ishihara, S.; Chang, S. S.; Bernstein, G.; West, E. D. Enthalpy and Heat-Capacity Standard Reference Material: Synthetic Sapphire (α-Al_2O_3) from 10 to 2250 K. *J. Res. Natl. Bur. Stand.* **1982**, *87*, 159−163.

(11) Dinsdale, A. T. SGTE Data for Pure Elements. *CALPHAD: Comput. Coupling Phase Diagrams Thermochem.* **1991**, *15*, 317−425.

(12) NIST Chemistry WebBook, NIST Standard Reference Database, No. 69, http://webbook.nist.gov/chemistry/; National Institute of Standards and Technology: Gaithersburg, MD, March 2003.

(13) Vasil'ev, I. A.; Korkhov, A. D. *Tr. Khim. Khim. Tekhnol., Gor'kii* **1974**, *36*, 103.

(14) Peppel, W. J. Preparation and Properties of the Alkylene Carbonates. *Ind. Eng. Chem.* **1958**, *50*, 767−770.
(15) Kolosovskii, N. A.; Udovenko, W. W. *Zh. Obshch. Khim.* **1934**, *4*, 1027.
(16) Chickos, J. S.; Acree, W. E., Jr.; Liebman, J. F. Estimating Solid−Liquid Phase Change Enthalpies and Entropies. *J. Phys. Chem. Ref. Data* **1999**, *28*, 1535−1673.
(17) Jones, A. R.; Aikens, D. A. Propylene Carbonate Cryoscopy. *J. Chem. Eng. Data* **1982**, *27*, 24−25.
(18) Hong, C. S.; Waksiak, R.; Finston, H.; Fried, V. Some Thermodynamic Properties of Systems Containing Propylene Carbonate and Ethylene Carbonate. *J. Chem. Eng. Data* **1982**, *27*, 146−148.
(19) Saunders, N.; Miodownik, A. P. *CALPHAD* (*Calculation of Phase Diagrams*): *A Comprehensive Guide*; Pergamon: London, 1998; Chapter 5.
(20) Gaskell, D. R. *Introduction to Metallurgical Thermodynamics*, 2nd ed.; Hemisphere: New York, 1981; Chapter 11.

Received for review July 11, 2003. Accepted November 2, 2003.

JE034134E